EVALUATION OF NONLINEAR BEHAVIOR OF CFRP LAMINATES IN TENSION AND COMPRESSION

Shunsuke Yoshida*, Tomohiro Yokozeki **, Toshio Ogasawara*, Shinji Ogihara***
*** Tokyo University of Science, ** The University of Tokyo,**
***** Japan Aerospace Exploration Agency**

Keywords: *Polymer-matrix composites, Plastic deformation, Nonlinear behavior, Loading-directional dependence*

Abstract

It is well known that fiber-reinforced composites exhibit nonlinear stress-strain response under off-axis loading. This nonlinear behavior is different in tension and compression. In this study, experimental characterization of unidirectional and angle-ply CFRP laminates is performed, and an unified description of the nonlinear behaviors in tension and compression is attempted by applying a simple plasticity model in which a pressure-dependent parameter is incorporated based on Sun and Chen's one-parameter plasticity model. Moreover, an attempt is made to predict the stress-strain behavior of angle-ply laminates using the simple plasticity model of the unidirectional laminates.

1 Introduction

It is widely recognized that fiber-reinforced composites exhibit nonlinear mechanical response under off-axis loading. Many studies have been conducted for the characterization of nonlinear behaviors of fiber-reinforced composites. Hahn and Tsai [1] predicted nonlinear stress-strain responses of unidirectional laminates under off-axis tensile loading using nonlinear elastic constitutive equations based on higher order energy functions. Sun and Chen [2] developed a one-parameter plasticity model to describe the nonlinear behavior of unidirectional composites. This model is based on a quadratic plastic potential and assumptions of plane stress state and no plastic deformation in the fiber direction. Ogihara et al. [3] applied this one-parameter plasticity model to characterize the nonlinear behaviors of angle-ply laminates.

Fiber-reinforced composites exhibit different nonlinear behaviors in tension and compression. In order to evaluate the mechanical response of composite materials, it is important to develop a unified model of composites in tension and compression. Therefore, in this study, experimental characterization and unified description of nonlinear behaviors are attempted by using a modified model [4] in which a pressure-dependent parameter is incorporated based on Sun and Chen's one-parameter plasticity model [2]. Moreover, an attempt is made to predict the stress-strain behavior of angle-ply laminates using the modified plasticity model of the unidirectional laminates.

2 Experimental procedure

2.1 Specimen

This study used a T800H/3633 carbon/epoxy system supplied by Toray Co. Ltd. Laminate configurations were unidirectional $[0]_{20}$ (for tension tests), $[0]_{40}$ (for compression tests) and angle-ply $[45/-45]_{2s}$. The respective resultant average thicknesses were 2.8 [mm], 5.7 [mm], and 1.1 [mm]. In order to measure the nonlinear behaviors under off-axis loading, off-axis specimens were prepared by cutting the specimens with off-axis angles of 15°, 30°, 45°, 60°, and 90° for unidirectional laminates.

2.2 Tension test

The monotonic tension tests of off-axis unidirectional specimens were performed using a mechanical testing machine (Instron 4482). The unidirectional specimens used for off-axis tension test have 120mm length and 10mm width. Oblique end tabs were adopted in reference to Sun and Chung [5] to measure accurate nonlinear stress-strain curves using small specimens. Back-to-back strain gages were attached to specimens in longitudinal and transverse directions. The applied crosshead speed was 1.5 mm/min.

The loading-unloading tension tests and the monotonic tension tests were performed in the case of angle-ply laminates. The angle-ply specimens used for tension tests have 200mm length and 12.5mm width with 50mm-length GFRP tabs bonded on both ends of the specimens. Back-to-back strain gages were attached to specimens in longitudinal and transverse directions. The applied crosshead speed was 2.0 mm/min. In the loading-unloading tension tests, the specimens were removed from the test machine after each cycle, and microscopic damages were observed using soft X-ray radiography.

2.3 Compression test

The monotonic compression tests were performed using the unidirectional laminates. The unidirectional specimens used for off-axis compression tests have 50mm length and 6mm width. Off-axis compression specimens were bonded to potting-type fixtures using epoxy adhesives. Compression loading was applied to the specimens using a supporting guide. Back-to-back strain gages were attached to specimens in longitudinal, transverse, and out-of-plane directions. The applied crosshead speed was 1.0 mm/min.

The monotonic compression tests of angle-ply laminates were also performed. The angle-ply specimens used for compression tests have 80mm length and 10mm width. Back-to-back strain gages were attached to specimens in longitudinal and transverse directions. Compression tests of angle-ply laminates were performed using a test jig consisting of an anti-buckling guide and clamping parts, and the applied crosshead speed was 0.3 mm/min.

3 Results and discussions

3.1 Unidirectional laminates

Fig. 1 shows the stress-strain curves for unidirectional laminates under off-axis tension and compression loading. It was found that the nonlinear behaviors are different in tension and compression. Table 1 shows the initial longitudinal Young's moduli, in-plane Poisson's ratios, and out-of-plane Poisson's ratios, which were evaluated using the experimental results in the strain range between 0.1% and 0.2%.

In this study, the modified plasticity model is applied for the description of nonlinear mechanical behaviors. In this model, Sun and Chen's one-parameter plasticity model [2] is extended to incorporate the loading-directional dependence. The effective stress is assumed to be in the following form inspired from the Drucker-Prager model.

Table 1. Obtained material properties for unidirectional laminates

Angle	Tension			Compression		
	E_x [GPa]	ν_{xy}	ν_{xz}	E_x [GPa]	ν_{xy}	ν_{xz}
15°	50.9	0.381	-	57.2	0.412	0.283
30°	21.1	0.352	-	22.9	0.395	0.328
45°	13.2	0.273	-	13.4	0.269	0.389
60°	10.5	0.175	-	10.4	0.155	0.444
90°	9.32	0.024	-	9.36	0.014	0.521

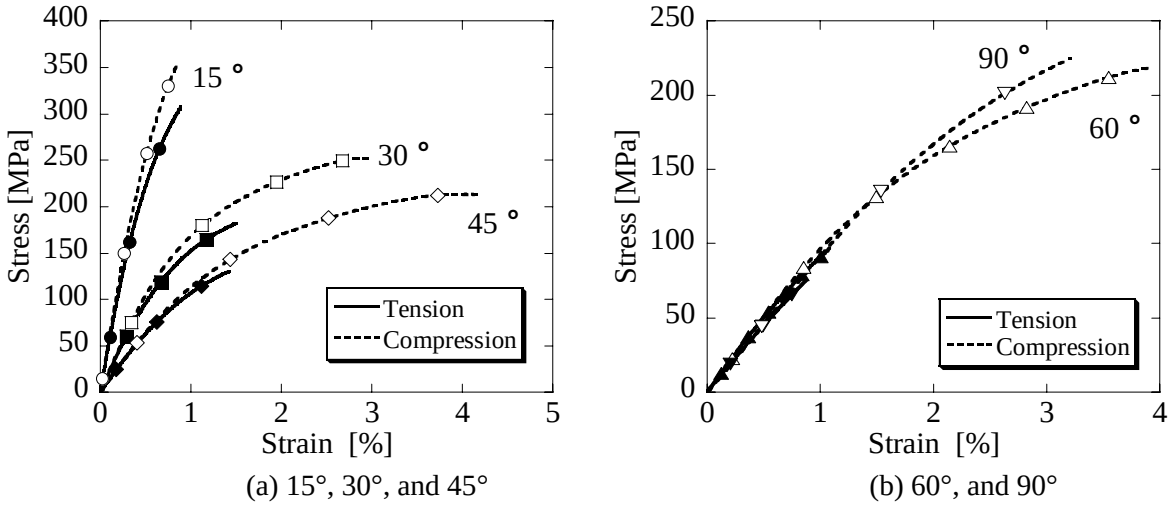

(a) 15°, 30°, and 45° (b) 60°, and 90°

Fig. 1. Longitudinal stress-strain curves for unidirectional laminates

$$\bar{\sigma} = \sqrt{\frac{3}{2}\left\{(\sigma_{22}-\sigma_{33})^2 + 2a_{66}\left(\tau_{12}^2+\tau_{13}^2\right)+2a_{44}\tau_{23}^2\right\}+a_1^2\sigma_{11}^2} + a_1(\sigma_{11}+\sigma_{22}+\sigma_{33}) \tag{1}$$

where a_{66} is the anisotropic parameter and a_1 is the loading-directional (pressure-dependent) parameter. In the case of plane stress state, the effective stress can be expressed as:

$$\bar{\sigma} = \sqrt{\frac{3}{2}\left(\sigma_{22}^2+2a_{66}\tau_{12}^2\right)+a_1^2\sigma_{11}^2} + a_1(\sigma_{11}+\sigma_{22}) = \tilde{\sigma}_{eff} + a_1(\sigma_{11}+\sigma_{22}). \tag{2}$$

The incremental plastic strain is expressed as

$$d\varepsilon_{ij}^p = \frac{\partial\bar{\sigma}}{\partial\sigma_{ij}}d\bar{\varepsilon}^p, \tag{3}$$

where $\bar{\varepsilon}^p$ is the effective plastic strain. Using Eqs. (1), (2), and (3),

$$\begin{Bmatrix} d\varepsilon_{11}^p \\ d\varepsilon_{22}^p \\ d\varepsilon_{33}^p \\ d\gamma_{12}^p \end{Bmatrix} = \begin{Bmatrix} \dfrac{a_1^2\sigma_{11}}{\tilde{\sigma}_{eff}}+a_1 \\ \dfrac{3\sigma_{22}}{2\tilde{\sigma}_{eff}}+a_1 \\ -\dfrac{3\sigma_{22}}{2\tilde{\sigma}_{eff}}+a_1 \\ 3a_{66}\dfrac{\tau_{12}}{\tilde{\sigma}_{eff}} \end{Bmatrix} d\bar{\varepsilon}^p \tag{4}$$

is obtained.

The material constants, a_{66} and a_1, and the effective stress-effective plastic strain relation are determined using the data of off-axis tension/compression tests. Let the (x-y) coordinate and the (1-2) coordinate, respectively, represent the global and the local (material principal) axes. Under uniaxial loading, the stresses in the local coordinate are expressed as:

$$\begin{aligned} \sigma_{11} &= \sigma_x\cos^2\theta \\ \sigma_{22} &= \sigma_x\sin^2\theta \\ \tau_{12} &= -\sigma_x\sin\theta\cos\theta \end{aligned} \tag{5}$$

where θ is the off-axis angle. The plastic strain in the global coordinate can be written as:

$$\begin{aligned} d\varepsilon_x^p &= d\varepsilon_{11}^p\cos^2\theta + d\varepsilon_{22}^p\sin^2\theta - d\gamma_{12}^p\sin\theta\cos\theta \\ d\varepsilon_y^p &= d\varepsilon_{11}^p\sin^2\theta + d\varepsilon_{22}^p\cos^2\theta + d\gamma_{12}^p\sin\theta\cos\theta \\ d\varepsilon_z^p &= d\varepsilon_{33}^p \end{aligned} \tag{6}$$

Substituting Eq. (4) into Eq. (6) with Eqs. (2) and (5) yields:

$$\begin{aligned} d\varepsilon_x^p &= \left(h(\theta)+a_1\right)d\bar{\varepsilon}^p \\ d\varepsilon_y^p &= \left(\frac{\left(\frac{3}{2}-3a_{66}+a_1^2\right)\sin^2\theta\cos^2\theta}{h(\theta)}+a_1\right)d\bar{\varepsilon}^p \\ d\varepsilon_z^p &= \left(-\frac{3}{2}\frac{\sin^2\theta}{h(\theta)}+a_1\right)d\bar{\varepsilon}^p \end{aligned} \tag{7}$$

where

$$h(\theta) = \begin{cases} \sqrt{\frac{3}{2}\sin^4\theta+3a_{66}\sin^2\theta\cos^2\theta+a_1^2\cos^4\theta} & (\sigma_x \ge 0), \\ -\sqrt{\frac{3}{2}\sin^4\theta+3a_{66}\sin^2\theta\cos^2\theta+a_1^2\cos^4\theta} & (\sigma_x \le 0). \end{cases} \tag{8}$$

From Eqs. (2), (5), and (7), the effective stress and effective plastic strain under uniaxial loading are

$$\bar{\sigma} = \left(h(\theta)+a_1\right)\sigma_x \tag{9}$$

$$\bar{\varepsilon}^p = \varepsilon_x^p / \left(h(\theta)+a_1\right) \tag{10}$$

Therefore, the effective stress and effective plastic strain can be expressed simply in terms of experimental values in off-axis tests. The effective stress-effective plastic strain relation depends on the choice of a_{66} and a_1. The values of the two parameters should be selected so that all curves derived from different off-axis specimens collapse into a single curve. The effective stress-effective plastic strain relation is approximated by the following power law:

$$\bar{\varepsilon}^p = A\bar{\sigma}^n. \tag{11}$$

Using Eq. (7), the in-plane and out-of-plane plastic Poisson's ratios are expressed as:

$$\nu_{xy}^p = -\frac{d\varepsilon_y^p}{d\varepsilon_x^p} = -\frac{\left(\frac{3}{2}-3a_{66}+a_1^2\right)\sin^2\theta\cos^2\theta+a_1h(\theta)}{h(\theta)\left(h(\theta)+a_1\right)} \tag{12}$$

$$\nu_{xz}^p = -\frac{d\varepsilon_z^p}{d\varepsilon_x^p} = -\frac{3}{2}\frac{\sin^2\theta+a_1h(\theta)}{h(\theta)^2+a_1h(\theta)} \tag{13}$$

The modified one-parameter plasticity model is applied to characterize the nonlinear behaviors of unidirectional laminates. It is assumed that the total strain at a certain level is decomposed into a linear elastic strain and a nonlinear strain, and the nonlinear part corresponds to plastic strain. Using the off-axis tension and compression test results, the effective stress-effective plastic strain relation and in-plane and out-of-plane plastic Poisson's ratios-off-axis angle relation were obtained, as shown in Fig. 2, Fig. 3, and Fig. 4. The parameters, a_{66} and a_1, were determined by minimizing the least-squares error of in-plane plastic Poisson's ratio curves in this study.

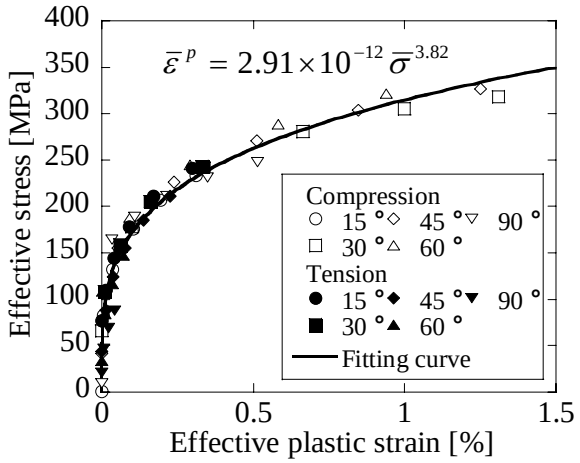

Fig. 2. Effective stress-effective plastic strain curves obtained from off-axis tests

Table 2. Elastic parameters obtained from off-axis tests results

a_{66}	a_1	A [MPa^{-n}]	n
3.1	0.09	2.91×10^{-12}	3.82

The obtained parameters are summarized in Table 2. The analytical stress-strain curves using the obtained parameters are compared with those using the experimental results (Fig. 5). The predicted results agree well with the experiments. It is demonstrated that the nonlinear response of unidirectional laminates in tension and compression can be predicted using the unified parameters based on the modified one-parameter model.

It is noteworthy that the presented method has potential to predict nonlinear behaviors under arbitrary in-plane loading using only tension or compression test results. Because this point is important for practical use, a further examination is necessary.

3.2 Angle-ply laminates

Fig. 6 shows stress-strain curves for angle-ply laminates under tension and compression loadings. The nonlinear behavior of the angle-ply laminates is different in tension and compression in comparison to the case of unidirectional laminates. It should be noted that the nonlinear behavior in monotonic loading is different from that in the loading-unloading case as shown in Fig. 6. Table 3 shows the initial longitudinal Young's moduli and in-plane Poisson's ratios, which were evaluated using the experimental results in the strain range between 0.1% and 0.2%.

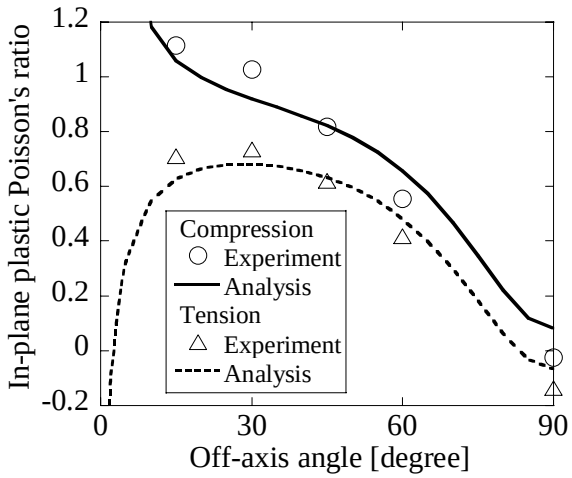

Fig. 3. Comparison of experimental and predicted in-plane plastic Poisson's ratio

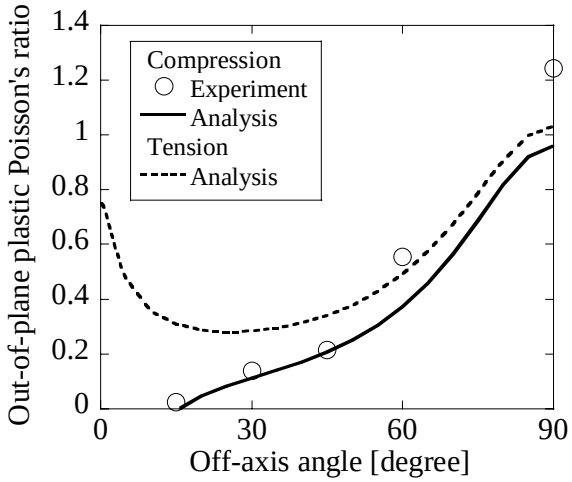

Fig. 4. Comparison of experimental and predicted out-of-plane plastic Poisson's ratio

In this study, an attempt is made to predict the stress-strain relations of angle-ply laminates by combining the modified one-parameter plasticity model and the classical lamination theory. The total strain increments are assumed to be the sum of the elastic strain increments and the plastic strain increments. The elastic and plastic strain increments obey the orthotropic linear stress-strain relations and the modified one-parameter plasticity model, respectively.

Table 3. Elastic parameters obtained for angle-ply laminates under compression and tension loading

Tension		Compression	
E_x [GPa]	ν_{xy}	E_x [GPa]	ν_{xy}
19.4	0.77	18.7	0.80

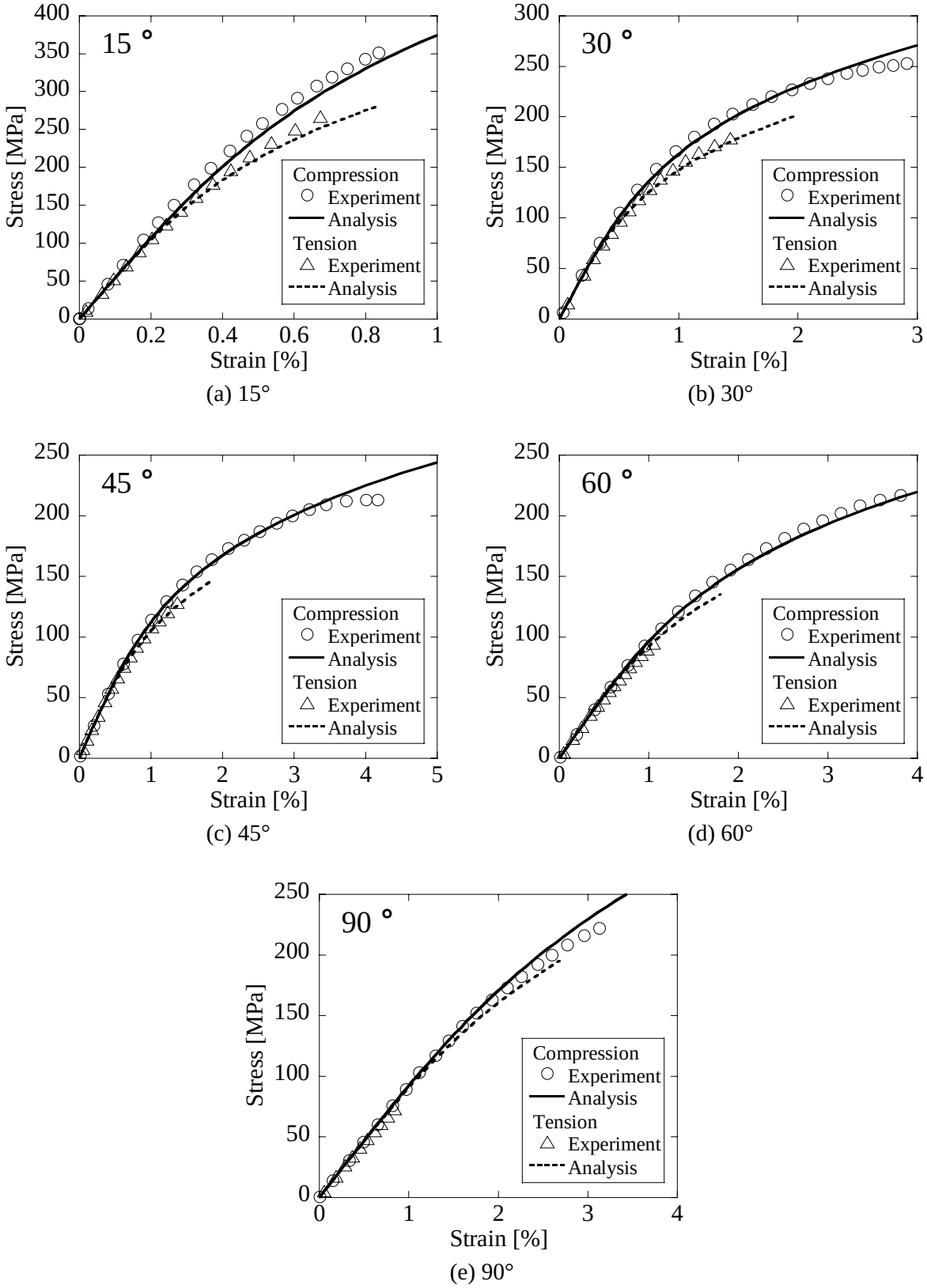

Fig. 5. Comparison of experimental and predicted stress-strain curves under compression and tension loading

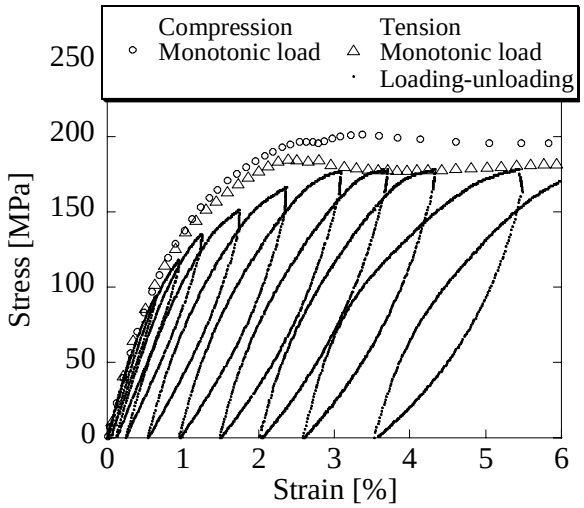

Fig. 6. Longitudinal stress-strain curves for angle-ply laminates under compression and tension loading

The total incremental stress-strain relations can be expressed as:

$$\begin{Bmatrix} d\varepsilon_{11} \\ d\varepsilon_{22} \\ d\gamma_{12} \end{Bmatrix} = \left[\left(S^e\right) + \left(S^p\right) \right] \begin{Bmatrix} d\sigma_{11} \\ d\sigma_{22} \\ d\tau_{12} \end{Bmatrix} \tag{14}$$

where

$$\left[S^e\right] = \begin{bmatrix} 1/E_1 & -\nu_{12}/E_1 & 0 \\ & 1/E_2 & 0 \\ sym & & 1/G_{12} \end{bmatrix} \tag{15}$$

$$\left[S^p\right] = An\bar{\sigma}^{n-1} \begin{bmatrix} S_{11}^p & S_{12}^p & S_{16}^p \\ & S_{22}^p & S_{26}^p \\ sym & & S_{66}^p \end{bmatrix} \tag{16}$$

$$\begin{aligned} S_{11}^p &= \left(\frac{a_1^2 \sigma_{11}}{\tilde{\sigma}_{eff}} + a_1 \right)^2, \quad S_{12}^p = \left(\frac{a_1^2 \sigma_{11}}{\tilde{\sigma}_{eff}} + a_1 \right) \left(\frac{3\sigma_{22}}{2\tilde{\sigma}_{eff}} + a_1 \right) \\ S_{16}^p &= 3a_{66} \frac{\tau_{12}}{\tilde{\sigma}_{eff}} \left(\frac{a_1^2 \sigma_{11}}{\tilde{\sigma}_{eff}} + a_1 \right), \quad S_{22}^p = \left(\frac{3\sigma_{22}}{2\tilde{\sigma}_{eff}} + a_1 \right)^2 \\ S_{26}^p &= 3a_{66} \frac{\tau_{12}}{\tilde{\sigma}_{eff}} \left(\frac{3\sigma_{22}}{2\tilde{\sigma}_{eff}} + a_1 \right), \quad S_{66}^p = 9a_{66}^2 \frac{\tau_{12}^2}{\tilde{\sigma}_{eff}^2} \end{aligned} \tag{17}$$

Now a multidirectional laminate under in-plane loading is considered. The total incremental stress-strain relations for the *k*th lamina in the laminate can be expressed in the form in the local (material) coordinate system:

$$\left\{ d\varepsilon^k \right\} = \left[S\left(\sigma^k\right) \right] \left\{ d\sigma^k \right\} \tag{18}$$

where superscript *k* denotes *k*th lamina. In the global coordinate system,

$$\left\{ d\tilde{\varepsilon}^k \right\} = \left[\tilde{S}\left(\sigma^k\right) \right] \left\{ d\tilde{\sigma}^k \right\} \tag{19}$$

is obtained, where:

$$\left\{ d\varepsilon^k \right\} = \left[T_\varepsilon \right] \left\{ d\tilde{\varepsilon}^k \right\} \tag{20}$$

$$\left\{ d\sigma^k \right\} = \left[T_\sigma \right] \left\{ d\tilde{\sigma}^k \right\} \tag{21}$$

$$\left\{ \tilde{S}\left(\sigma^k\right) \right\} = \left[T_\varepsilon \right]^{-1} \left[S\left(\sigma^k\right) \right] \left[T_\sigma \right] \tag{22}$$

and $[T_\varepsilon]$ and $[T_\sigma]$ are coordinate transformation matrix for stress and strain, respectively. The laminate stress-strain relations and the ply stress and strain in the global coordinate system are:

$$\left\{ \varepsilon^{LAM} \right\} = \left\{ \tilde{\varepsilon}^k \right\} \tag{23}$$

$$\left\{ \sigma^{LAM} \right\} = \frac{\sum t_k \left\{ \tilde{\sigma}^k \right\}}{\sum t_k} \tag{24}$$

where the superscript *LAM* represents the multidirectional laminate and t_k is the thickness of the *k*th ply. Considering the above relations, the stress-strain behavior of a multidirectional laminate under in-plane loading can be obtained.

Fig. 7 shows the comparison of experimental (monotonic loading) and predicted stress-strain curves for angle-ply laminates. The parameters used for the prediction are shown in Table 4. Elastic properties are obtained from compression test results. The predicted results agree with the experimental results up to 1.5-2.0% strain. It was demonstrated that the present model can describe nonlinear behaviors of angle-ply laminates in tension and compression.

However, some disparity of stress-strain curves between prediction and experiment was observed beyond approximately 2.0% strain. From the X-ray observation, ply-level microscopic damages (i.e. matrix cracks) occur and accumulate beyond the strain of about 3% during the loading-unloading tension tests. Therefore, at least, the predicted results will not agree with the experimental results beyond the strain of 3%, because the present model doesn't account for microscopic damages. Moreover, the plateau stress-strain curves are recorded when the applied strain exceeds 2% and 3% strain in the monotonic tension and loading-unloading tension test, respectively, as shown in Fig. 6. Therefore, there is a possibility that the microscopic damage accumulation behaviors under monotonic loading are different from those under the loading-unloading condition, which might be a reason for the disparity of stress-strain

curves between the prediction and the experiment. To confirm this, detailed observation of microscopic damage in monotonic loading might be necessary. In addition, the analysis that considers the rotation of the fiber might be necessary at large strain levels, which is also a reason for the disagreement.

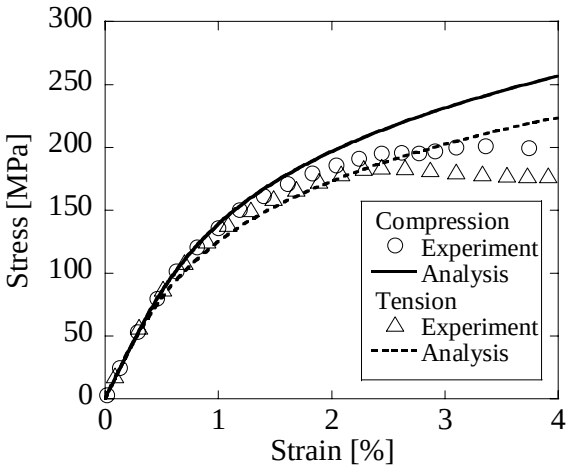

Fig. 7. Comparison of experimental and predicted stress-strain curves for angle-ply laminates

Table 4. Elastic parameters used to predict stress-strain relations of angle-ply laminates

E_1 [GPa]	136
E_2 [GPa]	9.36
ν_{12}	0.20
G_{12} [GPa]	5.30
a_{66}	3.10
a_1	0.09
A [MPa^{-n}]	2.91×10^{-12}
n	3.82

4 Conclusions

The nonlinear mechanical behavior of unidirectional laminates and the angle-ply laminates in tension and compression was evaluated experimentally. The modified one-parameter model was used to characterize the nonlinear response of unidirectional laminates in tension and compression. By combining the modified one-parameter plasticity model and the classical lamination theory, the stress-strain relation of angle-ply laminates could be predicted and compared with the experimental results. It is demonstrated that the present model can describe the different nonlinear behaviors in tension and compression for unidirectional and angle-ply laminates.

References

[1] Hahn HT. and Tsai SW. *Nonlinear elastic behavior of unidirectional composite laminate. J. Comp. Mater.*, Vol.7, pp.102-118, 1973.

[2] Sun CT. and Chen JL. *A Simple Flow Rule for Characterizing Nonlinear Behavior of Fiber Composites. J. Comp. Mater.*, Vol.23, pp.1009-1020, 1989.

[3] Ogihara S et al. *Characterization of nonlinear behavior of carbon/epoxy unidirectional and angle-ply laminates. J. Comp. Mater.*, Vol.11, pp.239-254, 2003.

[4] Yokozeki T et al. *Simple constitutive model for nonlinear response of fiber-reinforced composites with loading-directional dependence. Composites Science and Technology*, Vol.67, pp.111-118, 2007.

[5] Sun CT, and Chung I. *An oblique end-tab design for testing off-axis composite specimens. Composites*, Vol.24, pp.619-623, 1993.